Journal of Cellular Biochemistry 98:661–671 (2006)

LDL Induces Saos2 Osteoblast Death via Akt Pathways Responsive to a Neutral Sphingomyelinase Inhibitor

Benjamin Y. Klein,[1]* Zohar Kerem,[2] and Nathan Rojansky[3]

[1]Laboratory of Experimental Surgery, Hadassah University Hospital, Ein-Kerem, Jerusalem, Israel
[2]Institute of Biochemistry, Food Science and Nutrition, The Faculty of Agricultural, Food and Environmental Quality Sciences, The Hebrew University of Jerusalem, Rehovot, Israel
[3]Department of Obstetrics & Gynecology, Hadassah University Hospital, Ein-Kerem, Jerusalem, Israel

Abstract Atherosclerosis is epidemiologically associated with postmenopausal osteoporosis (OP) presumably by common etiologic factors, reflecting a state of co-morbidity in aging. Osteoblasts make a significant facet of this co-morbidity state. Since oxidized low-density lipoprotein (oxLDL) is a major factor in generation of vascular wall pathology, we examined the ability of native LDL (nLDL) and oxLDL to induce Saos2 osteoblasts growth arrest. OxLDL induced Saos2 cell death with morphological features of apoptosis that was inhibited mainly by caspase-9 and partially by caspase-3 but not by caspase-8 inhibitors. nLDL, like oxLDL, has induced cell death, where 60% ($P = 0.00033$) and 30% ($P = 0.075$, ns) of the cell death, respectively, could be inhibited by scyphostatin (a neutral sphingomyelinase [nSMase] inhibitor). Upon similar condition, nLDL inhibited the phosphorylation of Akt and two of its downstream targets, fork head receptor (FKHR) and glycogen synthase kinase-3 (GSK3). This is a pathway that stimulates cell survival and proliferation. nLDL has also induced an increase in the proapoptotic Bcl-Xs and it has diminished the potential antiapoptotic Src kinase activity. At the 4 h time-point, upon a substantial decrease in nLDL-induced Akt phosphorylation, scyphostatin has inhibited the reduction in FKHR and GSK3 phosphorylation but inexplicably not that of Akt. Scyphostatin has also corrected the reduction in Src kinase activity. Taken together, the results indicate that nLDL has induced apoptosis in Saos2 osteoblasts by inactivation of the pathway downstream to Akt using nSMase, and by involvement of Src kinase. Inferring that caspase-9 was the main executioner (rather than caspase-8 and-3) in Saos2 cell death, indicates that the nSMase-induced release of ceramide, directly activated the intrinsic mitochondrial apoptotic pathway. With regard to the Akt inactivation by nLDL, Saos2 osteoblasts responded in an opposite fashion to the response reported by others, in macrophages. J. Cell. Biochem. 98: 661–671, 2006.

Key words: LDL; osteoporosis; atherosclerosis; co-morbidity; Akt/PKB; Src-kinase; sphyngomyelinase

In recent years, a growing body of evidence is supporting the hypothesis that atherosclerosis (AS) and postmenopausal osteoporosis (OP) are two linked processes. The linkage between AS and OP was presented by epidemiological publications [Barengolts et al., 1998; Hak et al., 2000; Tanko et al., 2003] and may reflect a state of co-morbidity in aging. The possible biological links between OP and AS have been reviewed recently [Burnett and Vasikaran, 2002; McFarlane et al., 2004; Hamerman, 2005]. Several factors may link between AS and OP, for example, the mevalonate pathway [Garrett et al., 2001] that gives rise to end products like cholesterol that is a "passenger" of lipoproteins (that are involved in AS generation), or isoprenes used in prenylation of small GTPases which may be pro-osteoporotic. Isoprenes may also interact with PPAR-γ (peroxisome proliferator activator receptor γ), a transacting factor that can divert osteoprogenitors to the adipocyte lineage [Rzonca et al., 2004] and on the other hand, based on its agonistic effect and by an obscure mechanism, it participates in generating AS [Verrier et al., 2004]. There are signaling protein candidates that could induce bone-like matrix mineralization, mediated by

Grant sponsor: Israel Science Foundation; Grant number: 591/03.

*Correspondence to: Benjamin Y. Klein, Laboratory of Experimental Surgery, Hadassah University Hospital, Ein-Kerem, POB 12000 Jerusalem 91120, Israel.
E-mail: byklein@hadassah.org.il

Received 30 August 2005; Accepted 9 December 2005
DOI 10.1002/jcb.20807

vascular wall cells, and inversely, the loss of mineralized osteoid in bone itself. For example, Src kinase is essential for osteoclast activity [Boyce et al., 1992] and monocyte differentiation into macrophage-foam-cells in arterial intima [Cai et al., 2004] in contrast, subsiding of Src expression in osteoblasts [Klein et al., 1998] is important for osteoblast differentiation and, therefore, for bone formation [Marzia et al., 2000]. High-density lipoprotein (HDL) that removes excessive cholesterol from peripheral cells, has shown an anti-alveolar bone resorption activity [Jonarta et al., 2002], and has been shown to induce osteoclast apoptosis and to act against AS [Francis and Perry, 1999; Fazio and Linton, 2003; Spieker et al., 2004]. On the other hand, low-density lipoprotein (LDL) inhibits osteoblast growth [Klein et al., 2003] and participates in AS generation [Kita et al., 2001; Vasankari et al., 2001]. All these compounds act as factors, which are responsible for opposing biological processes relevant to OP versus AS. We have shown that LDL, oxidized (oxLDL) or native (nLDL), inhibit osteoblast cell line growth by different intensities, they can induce osteoblastic apoptosis, affect the Bcl-2/Bax anti-apoptotic ratios and Src kinase activity [Klein et al., 2003]. However, the signaling pathway/s through which LDL induces growth arrest in osteoblasts is awaiting more studies in order to discern targets in osteoblasts shared with vascular and bone cells. It is also reasonable to look for compounds (preferably food-derived) that could antagonize the osteoblast killing activity of LDL. Ideally, one should identify in osteoblasts targets that are common among signaling pathways within vascular cells and that respond to LDL. It has been shown that oxLDL inhibits apoptosis in macrophages [Hundal et al., 2001] and induces proliferation in vascular smooth muscle cells (SMC) [Auge et al., 2002] both via the Akt/PKB pathway activation and sphingolipid signaling. This mitogenic stimulation is in accord with the dependence of bone resorbing osteoclasts on lipoprotein-derived cholesterol for their generation, function, and survival [Luegmayr et al., 2004]. It also fits into the opposite osteoblast response to LDL, as these two cell types are functional opponents. We, therefore, examined the level of Akt activation and three of its immediate downstream substrates in Saos2 osteoblasts exposed to LDL. We found that, unlike in macrophages [Hundal et al., 2001] and vascular SMC [Hundal et al., 2001], in these osteoblast cells LDL inhibited the activation of the Akt and its sub-pathways.

MATERIALS AND METHODS

Reagents

Anti-Bcl-2 and anti-Bax antibodies were purchased form Upstate Biotechnology (Lake Placid, NY). Anti-phosphorylated Src antibodies (anti-pY529 and pY418) were purchased from BioSource Int (The Netherlands). Src protein was detected by mAb 327 [Lipsich et al., 1983]. Anti-Bcl-X antibodies were from Santa Cruz Biotechnology, anti-pT308Akt, anti-pS21/9GSK3, anti-pT1462tuberin, and anti-pS256FKHR were from Cell-Signaling Technology. Peroxidase-conjugated second antibodies were purchased from Jackson Immuno Research Laboratories, Inc. (West Grove, PA) fetal calf serum (FCS) was purchased from Life Technologies Laboratories (Grand Island, NY). Scyphostatin originates from Sankyo (Tokyo, Japan). Tissue culture reagents; tissue culture media, antibiotics, and trypsin-EDTA were purchased from Biological Industries, (Bet Haemek, Israel). Permeable caspase inhibitors DEVD (3), IETD (8), and LEHD (9) were from Biosource (Camarillo, CA).

Cell Culture

Saos2 osteoblastic cell line was cultured in maintenance medium Dulbecco's modified Eagle's medium (DMEM) supplemented with 10% FCS, antibiotics, and 10 mM glutamine. For experiments of cell-growth, kinetics cells were seeded in 96-well microtiter plates 5×10^3 cells/well in groups of 10 wells for each time point as indicated in each figure. Cells were then cultured for 24 h in maintenance medium subsequently either nLDL, oxLDL, control dialysis fluids, $CuSO_4$, or carrier were added in fresh DMEM medium at indicated concentrations as specified in each legend. The LDL was added at 1:10 dilution and indicated protein concentration. Cells were counted 48 h after exposure, following LDL addition using the methylene blue staining method.

Quantitative Cell Staining

Cells were stained using the methylene blue (MB) method, the plates were fixed in 0.5% glutaraldehyde for 30 min, rinsed with distilled water, and air dried overnight. Borate buffer

(0.1 M boric acid brought to pH 8.5 with NaOH) 0.2 ml/well, was added to the cells for 2 min and rinsed with tap water. Cells were then incubated in 0.1 ml of 1% MB in borate buffer for 60 min at room temperature, rinsed exhaustively with water, and air dried. The MB was then eluted from the stained cells by incubation with 0.2 ml of 0.1 N HCl at 37°C for 60 min. Optical density (OD) of the eluted MB was measured at 620 nm by an ELISA reader.

Electrophoresis and Western Blot Development

Cells were seeded, 2×10^4/well, in 6 cm diameter dishes, 24 h later LDL-containing medium at 1:10 dilution, or the post-LDL dialysis fluid of the same LDL sample that was treated similarly to the LDL. Cells were harvested for electrophoresis on indicated time point by cell lysis. Dishes set on ice, were washed twice with 6 ml of cold PBS removing washing solution to dryness. Ice-cold electrophoresis sample buffer (with 7% 2-mercaptoethanol and 3% sodium dodecylsulfate [SDS]) 50 or 100 μl was added to each dish and incubated on ice for 5 min. The lysates were quickly scraped off the plastic with a rubber policeman and transferred to cold tubes, boiled for 5 min, after removal of 10 μl for protein determination, they were cooled on ice and stored at −70°C until further use. Samples of 50 μg of lysed cultures were adjusted to equal volumes with plain sample buffer and fractionated by electrophoresis on 7–15% SDS-polyacrylamid gradient gels (SDS–PAGE). Gels were then electroblotted onto nitrocellulose filters that were blocked with 3% bovine serum albumin and 0.2% Tween 20 in PBS and divided into two half blots below the 38 kDa level. For phospho-c-Src detection and the phosphorylated Akt pathway, proteins filters were first incubated with anti-phosphorylated protein antibody and after washing, they were incubated with appropriate second antibody conjugated to peroxidase. The filters were exposed to ECL buffer to generate chemoilluminescence, by the activated peroxidase conjugates, detected by photo-radiography.

After radiography, the anti-phosphotyrosine antibodies were stripped off the filters and the above procedure was repeated with the appropriate antibody that recognizes unphosphorylated epitope in the same protein. The lower half blot was stained with mouse anti-Bcl-2 and several days later with rabbit anti-Bax Abs and rabbit anti-Bcl-X which recognizes both splicing variant. Stripping was performed by incubation of the filters in 62.5 mM Tris-HCl pH 6.7, 100 mM 2-mercaptoethanol, and 2% SDS for 30 min in a water bath shaking at 50°C.

Protein Determination

Duplicates of 5 μl electrophoresis sample were spotted onto 3-mm filter papers cut in pieces of 1 cm^2, dried, and stained with 2 mg/ml Coomassie blue for 20 min, destined with 40% methanol, 10% acetic acid until clearing of the unstained background, the stained protein spots staining dye was eluted with 3% SDS, protein quantities determined by Coomassie blue optical density at 620 nm compared with a similarly treated and serially diluted BSA standard.

Lipoprotein Isolation

LDL was isolated from LDL apheresis cartridges immediately after their consumption in the treatment of persons, homozygote in respect to hyperlipidemia. The use of cartridges designated for disposal was approved by the Helsinki committee for human experimentation. Removal of the LDL from the column was done by high ionic strength elution [Tani, 2000]. These cartridges were of the Kaneka brand having 400 ml bed volume (Liposorber LA40, Kaneka Corporation Osaka, Japan). Immediately after the apheresis session, the cartridges were washed with one bed volume of saline containing 2 mM EDTA and then eluted with increasing NaCl concentrations 0.3–0.5 M NaCl buffed with 50 mM phosphate pH7.4. To follow NaCl concentrations in various fractions, samples were measured for conductivity against known NaCl solutions. For additional purification, we modified a published method [Chung et al., 1980]. The eluted fractions were mixed with 0.7 g/ml KBr, rotated for 1 h at 4°C and 13 ml of the KBr-saturated LDL were placed at the bottom of Quick-Seal polyallomer tubes #342414 (Beckman, Palo Alto, CA) of 34 ml total volume each. The LDL was overlaid with 21 ml of PBS. The samples were spun for 3 h at 10°C in a VTi50 rotor, 45,000 rpm (170,000*g*). The tubes were subjected to fraction collection from the bottom or by needle aspiration through lateral puncture, for specific visible fractions. The LDL was dialyzed against 2 mM EDTA.

LDL Oxidation

Oxidation of LDL was carried out by incubation of 2 ml LDL adjusted to 10 μM $CuSO_4$ for 3 h in a gently shaking 37°C water bath. The nLDL was treated similarly but without $CuSO_4$. Both kinds of LDL samples were quantified by protein measurement. The dialysis fluids of each batch were saved for the use as control carries in the comparative tissue culture experiments. Before adding the LDL to the culture medium, it was adjusted to 2 mM $CaCl_2$ to neutralize traces of EDTA.

Statistical Methods

Where the differences of compared results were not clear a Student's *t*-test was performed mostly for paired samples or independent samples.

RESULTS

LDL Inhibition of Saos2 Osteoblast Cultures

LDL, native or oxidized, at the range of 1–2 mg/ml decreases Saos2 osteoblasts cell counts (see for example Table I). oxLDL has decreased Saos2 osteoblast cell counts, accompanied by features of apoptosis such as lobulated or pyknotic nuclei and apoptotic bodies (Fig. 1b). To obtain a general indication about the main pathways involved in the LDL-induced Saos2 growth arrest/apoptosis, we used the standard 100 μM concentration of inhibitors for three strategic caspases (caspase-9, 8, and 3). Figure 2 shows that in oxLDL-induced growth arrest, the most extensive correction has been achieved by the caspase-9 inhibitor, as opposed to the minimal inhibition achieved by the caspase-8 inhibitor. The caspase-3 inhibitor has shown an intermediate result. This indicates that oxLDL activates the intrinsic mitochondrial apoptotic pathway and/or a post mitochondrial activation of caspase-9, which resulted also in the next in-sequence activation of caspase-3. LDL can trigger release of ceramide from the plasma membrane due to neutral sphingomyelinase (nSMase) cleavage of sphingomyelin, and the released ceramide can activate the mitochondrial apoptotic pathway. To obtain a clue about the extent of the involvement of this apoptotic pathway in the Saos2 growth arrest, we have used scyphostatin, an nSMase-specific inhibitor [Nara et al., 1999], in osteoblast cultures exposed to LDL. Figure 3 shows that both oxLDL and nLDL can induce growth arrest in Saos2 osteoblasts, and that scyphostatin antagonized this LDL-induced growth arrest at the low doses with a biphasic mode. Both nLDL and oxLDL showed a similar biphasic pattern of response to scyphostatin that at 3 μM has corrected 60% of the growth arrest induced by nLDL, more than twofold the correction achieved by 1.5 μM (30%) against the oxLDL effect.

Akt Inactivation by nLDL

The direct induction of Saos2 osteoblast growth arrest via the mitochondrial pathway by LDL interaction with the cells and the possible triggering of the ceramide pathway lead us to test the Akt pathway. This is because the above result pointed towards a possible lipids interference with phospholipids that may have triggered cell signaling via phosphatydyl inositol kinase through the PI3K/Akt pathway. To test the extent of Akt pathway inactivation in Saos2 osteoblasts following their exposure to LDL, we extracted proteins, at three time points, from cultures exposed to a 1:10 dilution of nLDL. The proteins were fractionated by SDS–PAGE and activated Akt/PKB was detected on Western blots, in addition to proteins that represent three different sub-pathways downstream to phosphorylated (active) Akt. Figure 4A shows that phospho-Akt has been

TABLE I. Dose Response of Saos2 Osteoblasts Cell Counts to Native and Oxidized LDL

	oxLDL (n=10/sample)		nLDL (n=12/sample)		
Parameters	Mean	Significance[a]	Parameters	Mean	Significance
Carrier[b] effect	1.062 ± 0.035	$P = 0.602$	Carrier effect	1.0 ± 0.029	n.s.
1:40/carrier	1.043 ± 0.019	$P = 0.00028$	1:54/carrier	1.124 ± 0.021	$P = 0.0006$
1:20/carrier	0.936 ± 0.026	$P = 0.0011$	1:18/carrier	1.082 ± 0.038	$P = 0.0119$
1:10/carrier[c]	0.722 ± 0.020	$P = 1.67E\text{-}07$	1:6/carrier	0.521 ± 0.026	$P = 3.84E\text{-}09$

[a]Paired *t*-test 2 tail.
[b]Carrier for nLDL = last dialysis fluid, and for oxLDL dialysis fluid + $CuSO_4$ (10 μM).
[c]1:10 LDL = 1.4 mg/ml protein equivalent for LDL.

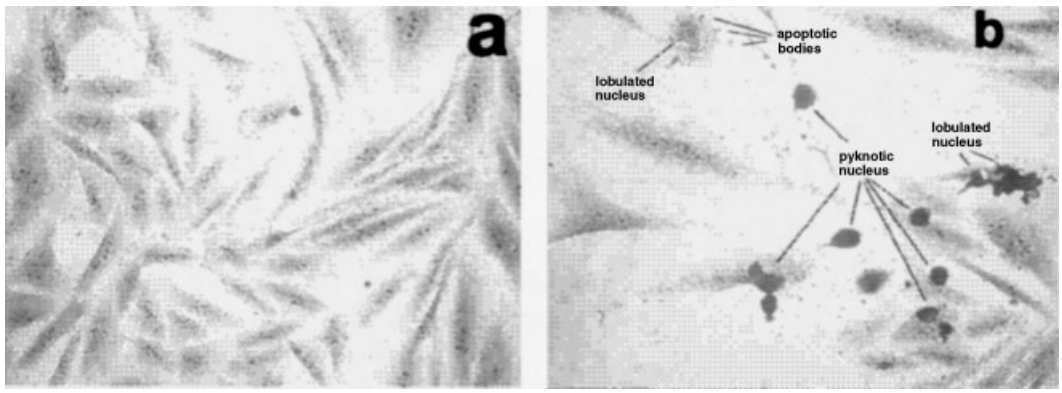

Fig. 1. Morphology of Saos2 osteoblasts exposed to oxLDL for 48 h. Saos2 cells were seeded ($1.5 \times 10^4/cm^2$), 24 h later, the medium was replaced with fresh medium 1:10 LDL dialysis fluid (**a**) and 1:10 oxLDL:medium v/v (**b**). Both the post LDL dialysis fluid and the LDL were treated with 10 μM $CuSO_4$ for 3 h at 37°C before use (3.7 mg protein/ml concentration in culture). After exposure of 48 h to oxLDL, the cells were fixed with 0.5% glutaraldehyde, stained with methylene blue, and photographed under an inverted microscope (magnification = 1 × 200). Note the lobulated and pyknotic nuclei and apoptotic-bodies in panel b.

diminished relatively to the control cells already after 1 h but its fall was dipper after 4 h, which is also seen in the quantitative bar chart for which the bands were corrected in reference to the β-actin bands (Fig. 4B). The Fork Head receptor (FKHR) that downregulates responses to growth factors in its unphosphorylated state was kept active as a cell cycle inhibitor (in its unphosphorylated state) in response to nLDL, presumably due to inactivation of Akt. Tuberin that by phosphorylation at threonine1462 inhibits translation via inhibition of

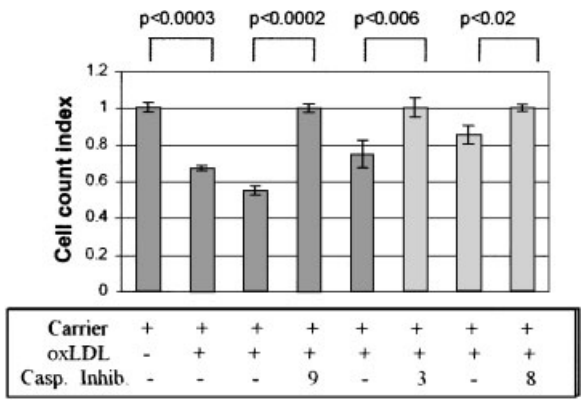

Fig. 2. Differential rescue of Saos2 cells by inhibitors of caspase-9, 3, and 8. Saos2 cells were seeded in 96-well plates at 5×10^3cells/well and after 24 h, the medium was replaced with fresh medium containing either 100 μM cell-permeable caspase inhibitors or their solubilization carrier (DMSO). After 1 h incubation, an equal volume of medium was added to all wells containing 20% oxLDL (10% final, as in Fig. 1), except the untreated controls to which post-LDL dialysis fluid was added. The cultures were fixed and stained with methylene blue for colorimetric cell count. The untreated and the caspase-inhibited cultures were adjusted to unity and indices for the oxLDL alone were calculated accordingly. Statistical significance was derived by the paired *t*-test between inhibited and uninhibited cultures, matching each culture with its localization opponent in the plate (n = 10).

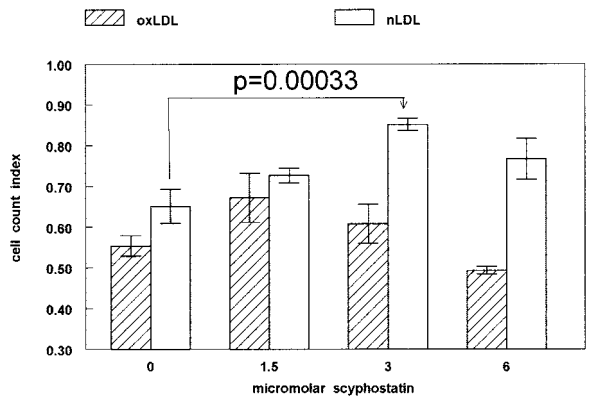

Fig. 3. Scyphostatin inhibition of LDL-induced osteoblast cell death. Saos2 osteoblast were seeded as in Figure 2 and after 24 h, the medium was replaced with fresh medium containing either scyphostatin serial dilutions or equivalent dilutions of its carrier (ethanol). Subsequently an equal volume of nLDL or oxLDL was added to all wells apart from the control group with 0 scyphostatin. After 48 h, the cells were fixed, stained, and counted. Each bar represents an index between each experimental and its own uninhibited group of wells (n = 10 indices/bar). Scyphostatin (3 μM) inhibited the nLDL-induced reduction in cell count relative to 0 μM scyphostatin ($P = 0.00033$). Effects of the other concentrations were also positive but not statistically significant (for 1.5 μM $P = 0.091$, for 6.0 μM $P = 0.108$). The effect of the highest ethanol carrier concentration relative to untreated was 1.046 ± 0.164. Scyphostatin inhibited the effect of oxLDL non-significantly, (for 1.5 μM $P = 0.076$, for 3 μM $P = 0.317$), while 6.0 μM increased the oxLDL effect non-significantly ($P = 0.108$). In the oxLDL cultures, the effect of the highest ethanol carrier concentration relative to untreated cultures was 1.002 ± 0.026.

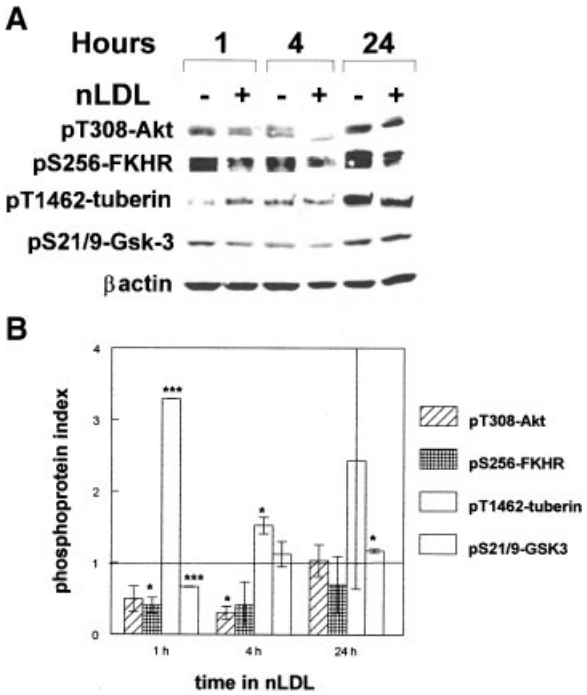

Fig. 4. Akt pathway phosphorylation response to nLDL. Saos2 osteoblasts were seeded in 25 cm^2 flasks (10^4 cells/cm^2) and 24 h later, the medium was replaced with 1:10 dilution of nLDL or post-LDL dialysis buffer. At indicated time-points, proteins from pairs of flasks (nLDL and dialysis buffer controls) were harvested and run on SDS–PAGE for immunoblots preparation. The blots were reacted with indicated antibodies and developed (**A**). The scanned densities of all bands were normalized against the β-actin of their lane. Each band is expressed as an index relative to its proper nLDL-untreated control, unity represents the level of no-change (**B**).

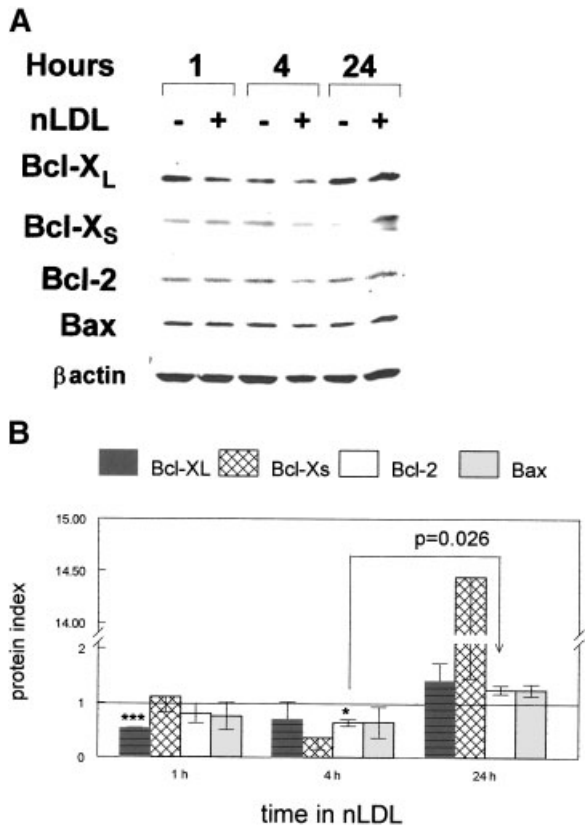

Fig. 5. Bcl-2 family proteins response to nLDL. The lower molecular size portion of immunoblots prepared (as in Fig. 4) were reacted with indicated antibodies (**A**). The scanned bands were treated as in Figure 4 (**B**).

mammalian target of rapamycin (mTOR) has shown an early activation (after 1 h under nLDL) relative to the control cells. This active state of tuberin became equal to its state in the control cells after 4 h in spite of the deepest Akt inactivation at this time point. Glycogen synthase kinase-3 (GSK3) showed a relatively lower phosphorylation at serine 21 and 9 more so at 1 than at 4 h, this may have enabled it an early contribution to cell cycle inhibition. The phosphorylation of GSK3 resumed in parallel with the reactivation of Akt at the 4 and 24 h time points.

Bcl-2 and Bcl-X Response to nLDL

An early decrease in the index of the anti-apoptotic Bcl-X_L took place 1 h after exposure to nLDL (Fig. 5A), which was accompanied by a slight relative increase in the pro-apoptotic Bcl-Xs. This has recovered at the 4 h time point but the pro-apoptotic ratio resumed at the 24 h time point (Fig. 5B). The Bcl-2 anti-apoptotic protein showed a decrease only at the 4 h time point while its pro-apoptotic opponent (Bax) quantity did not change relative to β-actin.

Src Activity Response to nLDL

The c-Src protein responded to nLDL by a decrease at the 1 and 4 h time points, which has been inverted at the 24 h time point (Fig. 6A). The ratio between phosphorylation states of tyrosine418 and tyrosine529, in the human Src protein, indicate the level of Src kinase activity. The bar chart demonstrates that the nLDL-induced decrease in Src activity index (Fig. 6B) resulted from the loss of protein phosphorylated on the tyrosine418 (kinase activation site) rather than the gain of molecules predominantly phosphorylated on the inactivation site on tyrosine529. This pattern is valid for the 1 and 4 h time points but completely changes at the 24 h time point. nLDL induced a relative gain in the Src protein, Figure 6B indicates that

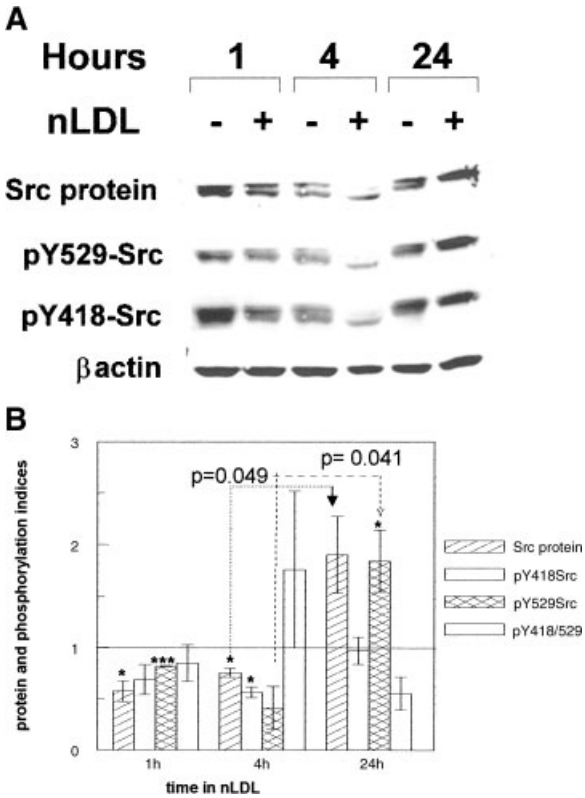

Fig. 6. Activity of c-Src kinase in response to nLDL. Immunoblots of proteins from Saos2 cells exposed to nLDL, prepared as in Figure 4 were generated with various anti-Src proteins antibodies in between stripping procedures (**A**). The bar chart (**B**) shows the β-actin-corrected bands as compared between nLDL-treated and untreated cultures.

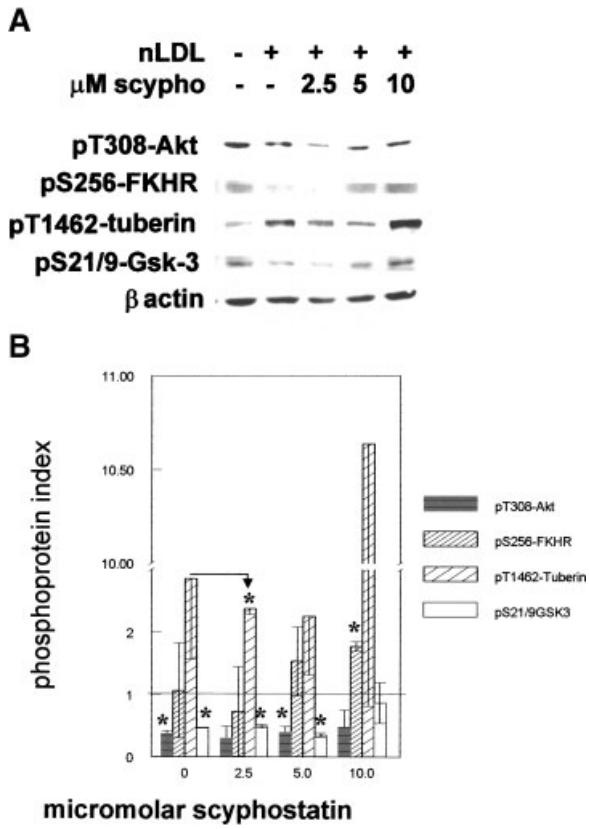

Fig. 7. Recovery of phosphoproteins downstream to Akt from nLDL-induced inhibition by treatment with scyphostatin. Saos2 osteoblasts seeded as in Figure 4 were first treated with indicated concentrations of scyphostatin 10 min before addition of nLDL. All the cultures were harvested after 4 h and processed as described in the legend of Figure 4. Immunoblots with antibodies recognizing Akt pathways phosphoproteins are shown in **A**. Quantitative bar chart is shown in **B**.

this gain was accompanied by a higher portion of the kinase-inactivating tyrosin529 phosphorylation versus a concomitant loss of the phosphorylation of the kinase-activating tyrosine418.

The nLDL-inhibited Akt Response to Scyphostatin

We selected the 4 h time point after Saos2 osteoblasts exposure to nLDL in which the Akt reached a substantial inactivating dephosphorylation, to follow the effect of scyphostatin. Figure 7A shows that although 3 μM scyphostatin resulted in substantial correction of the Saos2 osteoblast growth arrest induced by nLDL, a very similar dose (2.5 μM) did not inhibit the decrease in Akt protein phosphorylated at its threonine308, it has rather enabled its further decrease. Yet the FKHR state of serine256 phosphorylation has been increased with 5 and 10 μM scyphostatin, which is expected to relieve the cell cycle arrest. Only the 5 μM dose of scyphostatin has decreased the phosphorylated tuberin protein which should enable relieve of the inhibition of protein synthesis via mTOR. GSK3 shows a straightforward dose response in its serine21/9 phosphorylation (Fig. 7A,B) that has resulted from the scyphostatin treatment, which shows a clear correction of the nLDL-induced GSK3 unphosphorylated state.

Bcl-2 and Bcl-X Response to Scyphostatin in the Presence of nLDL

The absolute quantity of Bcl-2 and Bax decreased 4 h after exposure to nLDL (Fig. 8A) as occurred also to Bcl-X_L. Scyphostatin treatment is accompanied by a minute recovery of these proteins but upon β-actin normalization, the ratios of Bax/Bcl-2 and those of Bcl-Xs/Bcl-X_L did not surpass the unity level (Fig. 8B). These results indicate that Bcl-2 family protein

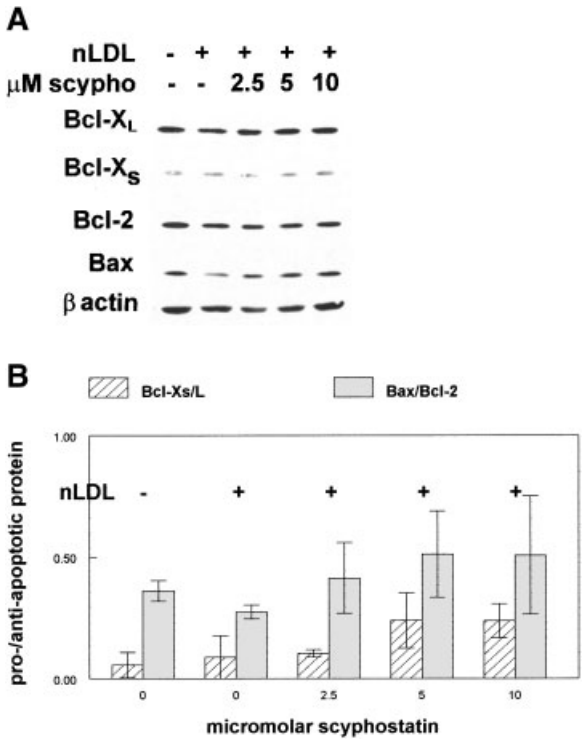

Fig. 8. Response to nLDL of pro/anti-apoptotic ratios of Bcl-2 family protein and the change by scyphoatatin. Immunoblot shown in (**A**) and bar chart in **panel B**.

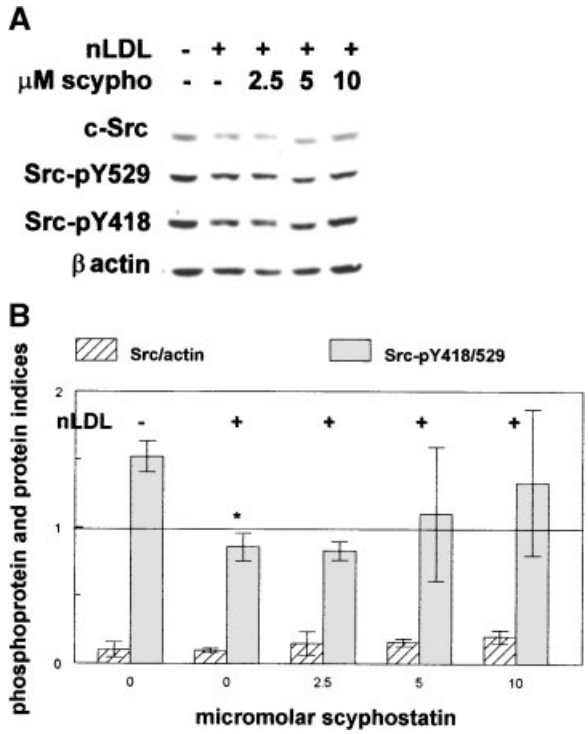

Fig. 9. Correction of c-Src kinase activity by scyphostatin. Immunoblot with various anti-c-Src antibodies shown in **panel A** and the quantitative bar chart is shown in **panel B**.

response at the 4 h time point is irrelevant to the scyphostatin inhibition of the nLDL-induced growth arrest.

Src Kinase Activity Response to Scyphostatin in the Presence to nLDL

The Src protein showed a decrease in tyrosine418 phosphorylation that was not accompanied by change in the phosphorylation of tyrosine529 (Fig. 9A). After quantitative normalization with β-actin and plotting of Src kinase activity ratios (Fig. 9B), it can be seen that 5 μM scyphostatin were sufficient to antagonized the decreased kinase activity ratio induced by nLDL.

DISCUSSION

As far as the response of osteoblasts to LDL is concerned we cannot as yet categorically state that the oxidation is the most important factor in the response of these cells to LDL. In fact, it has been shown that in vascular SMC, mild oxidation is sufficient for activation of numerous apoptotic signals [Napoli et al., 2000]. We have used nLDL which had an effect on the osteoblasts similar to that of the oxLDL [Klein et al., 2003]. Similarly, in the present work, both nLDL and oxLDL induced growth arrest in Saos2 osteoblasts. The inhibition of caspases in cultures of Saos2 osteoblasts exposed to oxLDL resulted in a similar outcome as obtained by others [Kume and Kita, 2004] in vascular SMCs. These authors claimed that caspase-9 and 3 were activated by oxLDL via lectin-like oxLDL receptors (Lox-1) that has induced mitochondrial cytochrom-c release, in parallel the oxLDL inhibited P3IK/Akt. The option of nSMase activation via Fas receptor to release ceramide [Suzuki et al., 2003] (while bypassing activation of caspase-8) lead us to inhibit nSMase in the presence of oxLDL or nLDL. Scyphostatin, the specific nSMase inhibitor, has indeed inhibited more than 60% of the nLDL (and only 30% of the oxLDL)-induced Saos2 osteoblast growth arrest, indicating that nLDL induction of growth arrest is to a great extent depending on nSMase activation. This is consistent with the reports that oxLDL inhibits acid sphingomyelinase (aSMase) [Hundal et al., 2001, 2003] probably more than it activates nSMase. Inhibition of one and activation of the other may

reconcile the different results obtained with oxLDL in macrophages [Hundal et al., 2001, 2003] and those obtained in endothelial cells [Chen et al., 2004]. Based on accumulated information on aSMase and nSMase and the quantitative differences that nSMase inhibition showed for oxLDL and nLDL (Fig. 3), this differential response might result from diverse reaction of these two SMases to a range of LDL oxidation. The substantial correction (with scyphostatin) of the cell counts decreased by nLDL raised the question as to how the Akt/PKB pathway would respond to the same nLDL. Akt was partially dephosphorylated already 1 h after exposure to nLDL and became even more so after 4 h. This Akt inactivation is consistent with result of others [Kume and Kita, 2004] that obtained it rather with oxLDL. FKHR and GSK3 responded to nLDL as would have been expected under Akt inhibition however, tuberin (TSC2) showed a response that was incongruent with the phosphorylation state of Akt. We expected that active Akt will phosphorylate tuberin on its threonine1462 and thereby induce negative control on mTor. A relationship of proper phospho-Akt to proper phospho-tuberin was seen only after 24 h of nLDL exposure, whereas at 1 h and 4 h time-points, tuberin remained phosphorylated in spite of Akt dephosphorylation. Tuberin could have been phosphorylated by a different kinase, for example, AMP-activated protein kinase (AMPK) that may phosphorylate tuberin. Such activation of tuberin may occur in response to an LDL-induced stress signal (of an unknown nature) in which LKB1 activates AMPK due to increased AMP/ATP ratios [Inoki et al., 2003]. It is however more likely that the aberrant phosphorylation of tuberin is related to the lack of p53 expression in these Saos2 cells. It is known [Karuman et al., 2001] that normally LKB1 is physically bound to p53 therefore the lack of p53 could have resulted in the uncontrolled phosphorylation of tuberin and a delay of signal termination by a proper phosphatase.

In parallel to Akt inactivation, exposure to nLDL was followed by a relative decrease in Bcl-X_L and an increase in Bcl-Xs, which was not seen at the 4 h time-point but has strongly reappeared after 24 h. This surge in Bcl-Xs/Bcl-X_L ratio, is consistent with a possible NFκB transcriptional activation of Bcl-X_L [Glasgow et al., 2001] under active Akt and a change to transcriptional activation of its splicing variant Bcl-Xs under inhibition of Akt, perhaps by unleashing GSK3 to inhibit Cylin-D1. Cyclin-D1 inhibition is associated with increased Bcl-Xs expression [Mihara et al., 2003]. Bax was overexpressed relative to Bcl-2 only at the 4 h time-point. Although these results do not indicate the intracellular localization, at least the Bcl-Xs can be regarded as a participant in cell death since its ratio to Bcl-X_L is not dependent on it ability to cause cell death [Heermeier et al., 1996]. We have also followed the Src kinase protein (pp60Src) because it is a balancing factor within bone tissue between bone resorption and bone formation. Osteoclasts largely depend on Src expression [Boyce et al., 1992] and osteoblast-differentiation depends on attenuation of its expression [Klein et al., 1998; Marzia et al., 2000]. Src is also anti-apoptotic and its kinase activity is clearly reduced after 24 h under nLDL in spite of the augmentation of its total protein. Note that phosphorylation of tyrosine519 in human Src by Csk (as opposed to tyrosine418) has an inactivation effect on Src kinase. Csk activity is also associated with activation of PI3K/Akt pathway [Zagozdzon et al., 2002; Gu et al., 2003; Dey et al., 2005]. This is consistent with reduction of the Src activity index but not with the increase in Src protein at the 24 h time point. In the surviving cells, (after 24 h) nLDL induced a relative gain in the Src protein (Fig. 6B), which indicates that this gain is accounted for by the portion of the kinase-inactivating tyrosin529 phosphorylation versus a concomitant loss of the phosphorylation of the kinase-activating tyrosin418. This may be interpreted as development of Src protein resistance to breakdown either because of an as yet obscure mechanism perhaps related to the c-Src molecule folding on it self (pY529 binding to its own SH3 domain). Alternatively, mitochondrial recovery from uncoupling and from cytochrome c release in the selectively surviving cells 24 h after the nLDL insult, could explain a gain in Src protein. It has been shown that an uncoupling agent can induce Src cleavage at a caspase-3 targeting motif about 30 A.A. from its c-terminus, which can be inhibited by the caspase-3 inhibitor [Karni and Levitzki, 2000]. Taken together, nLDL has set in motion several factors that slowdown cell metabolism, growth, and proliferation, and cause cell death. Most of this response is consistent with inhibition of the Akt signaling pathway. The growth arrest

occurred in spite of the fact that tuberin acted independently opposite to its normal response. We selected the 4 h time-point to test the inhibition of the nLDL effect because at this point Akt showed a clear decline in its phosphorylation. Interestingly, scyphostatin has inhibited (or corrected) the fall in FKHR and GSK3 and has even increased the tuberin phosphorylation dose dependently, in spite of the fact that Akt phosphorylation itself, which was inhibited by nLDL, was not corrected by scyphostatin. The appearance of the Bcl-2 family ratios at the 4 h time-point do not contribute to the understanding of the way that scyphostatin protected the Saos2 cells from nLDL growth arrest. On the other hand, Src kinase activity at the 4 h time point was corrected in parallel with scyphostatin treatment in the presence of nLDL while the Src protein quantity did not change. The correction of the positive activities of FKHR, Src-kinase, and the negative activity of GSK3 and the phosphorylation state of tuberin by scyphostatin was sufficient to prevent growth arrest. However, we cannot show that this was achieved via inhibition of the dephosphorylation of threonine308 in Akt. Whatever the reason for this unexplained phenomenon, it is clear that nLDL arrested the Saos2 osteoblast growth in parallel to inhibition of Akt activating phosphorylation and activation of at least two of its downstream effectors, which reverted in parallel to the inhibition of cell death. The importance of these findings is that they are diagonally opposed to the response of vascular macrophages to oxLDL, and thus underscore the possible generation of a co-morbidity mechanism causing bone and vascular pathology by similar inducers, namely LDL together with cellular elements of these tissues.

REFERENCES

Auge N, Garcia V, Maupas-Schwalm F, Levade T, Salvayre R, Negre-Salvayre A. 2002. Oxidized LDL-induced smooth muscle cell proliferation involves the EGF receptor/PI-3 kinase/Akt and the sphingolipid signaling pathways. Arterioscler Thromb Vasc Biol 22:1990–1995.

Barengolts EI, Berman M, Kukreja SC, Kouznetsova T, Lin C, Chomka EV. 1998. Osteoporosis and coronary atherosclerosis in asymptomatic postmenopausal women. Calcif Tissue Int 62:209–213.

Boyce BF, Yoneda T, Lowe C, Soriano P, Mundy GR. 1992. Requirement of pp60c-src expression for osteoclasts to form ruffled borders and resorb bone in mice. J Clin Invest 90:1622–1627.

Burnett JR, Vasikaran SD. 2002. Cardiovascular disease and osteoporosis: Is there a link between lipids and bone? Ann Clin Biochem 39:203–210.

Cai Q, Lanting L, Natarajan R. 2004. Growth factors induce monocyte binding to vascular smooth muscle cells: Implications for monocyte retention in atherosclerosis. Am J Physiol Cell Physiol.

Chen J, Mehta JL, Haider N, Zhang X, Narula J, Li D. 2004. Role of caspases in Ox-LDL-induced apoptotic cascade in human coronary artery endothelial cells. Circ Res 94:370–376.

Chung BH, Wilkinson T, Geer JC, Segrest JP. 1980. Preparative and quantitative isolation of plasma lipoproteins: Rapid, single discontinuous density gradient ultracentrifugation in a vertical rotor. J Lipid Res 21: 284–291.

Dey N, Howell BW, De PK, Durden DL. 2005. CSK negatively regulates nerve growth factor induced neural differentiation and augments AKT kinase activity. Exp Cell Res 307:1–14.

Fazio S, Linton MF. 2003. Apolipoprotein AI as therapy for atherosclerosis: Does the future of preventive cardiology include weekly injections of the HDL protein? Mol Interv 3:436–440.

Francis GA, Perry RJ. 1999. Targeting HDL-mediated cellular cholesterol efflux for the treatment and prevention of atherosclerosis. Clin Chim Acta 286:219–230.

Garrett IR, Gutierrez G, Mundy GR. 2001. Statins and bone formation. Curr Pharm Des 7:715–736.

Glasgow JN, Qiu J, Rassin D, Grafe M, Wood T, Perez-Pol JR. 2001. Transcriptional regulation of the BCL-X gene by NF-kappaB is an element of hypoxic responses in the rat brain. Neurochem Res 26:647–659.

Gu J, Nada S, Okada M, Sekiguchi K. 2003. Csk regulates integrin-mediated signals: Involvement of differential activation of ERK and Akt. Biochem Biophys Res Commun 303:973–977.

Hak AE, Pols HA, van Hemert AM, Hofman A, Witteman JC. 2000. Progression of aortic calcification is associated with metacarpal bone loss during menopause: A population-based longitudinal study. Arterioscler Thromb Vasc Biol 20:1926–1931.

Hamerman D. 2005. Osteoporosis and atherosclerosis: Biological linkages and the emergence of dual-purpose therapies. Qjm 98:467–484.

Heermeier K, Benedict M, Li M, Furth P, Nunez G, Hennighausen L. 1996. Bax and Bcl-Xs are induced at the onset of apoptosis in involuting mammary epithelial cells. Mech Dev 56:197–207.

Hundal RS, Salh BS, Schrader JW, Gomez-Munoz A, Duronio V, Steinbrecher UP. 2001. Oxidized low density lipoprotein inhibits macrophage apoptosis through activation of the PI 3-kinase/PKB pathway. J Lipid Res 42: 1483–1491.

Hundal RS, Gomez-Munoz A, Kong JY, Salh BS, Marotta A, Duronio V, Steinbrecher UP. 2003. Oxidized low density lipoprotein inhibits macrophage apoptosis by blocking ceramide generation, thereby maintaining protein kinase B activation and Bcl-XL levels. J Biol Chem 278: 24399–24408.

Inoki K, Zhu T, Guan KL. 2003. TSC2 mediates cellular energy response to control cell growth and survival. Cell 115:577–590.

Jonarta AL, Pudyani PS, Sosroseno W. 2002. Effect of high-density lipoprotein on lipopolysaccharide-induced alveolar bone resorption in rats. Oral Dis 8:261–267.

Karni R, Levitzki A. 2000. pp60(cSrc) is a caspase-3 substrate and is essential sfor the transformed phenotype of A431 cells. Mol Cell Biol Res Commun 3:98–104.

Karuman P, Gozani O, Odze RD, Zhou XC, Zhu H, Shaw R, Brien TP, Bozzuto CD, Ooi D, Cantley LC, et al. 2001. The Peutz-Jegher gene product LKB1 is a mediator of p53-dependent cell death. Mol Cell 7:1307–1319.

Kita T, Kume N, Minami M, Hayashida K, Murayama T, Sano H, Moriwaki H, Kataoka H, Nishi E, Horiuchi H, et al. 2001. Role of oxidized LDL in atherosclerosis. Ann NY Acad Sci 947:199–205; discussion 205-206.

Klein BY, Levitzki R, Ben-Bassat H. 1998. Src protein and tyrosine-phosphorylated protein profiles in marrow stroma during osteogenic stimulation. J Cell Biochem 69: 316–325.

Klein BY, Rojansky N, Ben-Yehuda A, Abou-Atta I, Abedat S, Friedman G. 2003. Cell death in cultured human Saos2 osteoblasts exposed to low-density lipoprotein. J Cell Biochem 90:42–58.

Kume N, Kita T. 2004. Apoptosis of vascular cells by oxidized LDL: Involvement of caspases and LOX-1 and its implication in atherosclerotic plaque rupture. Circ Res 94:269–270.

Lipsich LA, Lewis AJ, Brugge JS. 1983. Isolation of monoclonal antibodies that recognize the transforming proteins of avian sarcoma viruses. J Virol 48:352–360.

Luegmayr E, Glantschnig H, Wesolowski GA, Gentile MA, Fisher JE, Rodan GA, Reszka AA. 2004. Osteoclast formation, survival and morphology are highly dependent on exogenous cholesterol/lipoproteins. Cell Death Differ 11(Suppl 1):S108–S118.

Marzia M, Sims NA, Voit S, Migliaccio S, Taranta A, Bernardini S, Faraggiana T, Yoneda T, Mundy GR, Boyce BF, et al. 2000. Decreased c-Src expression enhances osteoblast differentiation and bone formation. J Cell Biol 151:311–320.

McFarlane SI, Muniyappa R, Shin JJ, Bahtiyar G, Sowers JR. 2004. Osteoporosis and cardiovascular disease: Brittle bones and boned arteries, is there a link? Endocrine 23:1–10.

Mihara M, Shintani S, Nakashiro K, Hamakawa H. 2003. Flavopiridol, a cyclin dependent kinase (CDK) inhibitor, induces apoptosis by regulating Bcl-X in oral cancer cells. Oral Oncol 39:49–55.

Napoli C, Quehenberger O, De Nigris F, Abete P, Glass CK, Palinski W. 2000. Mildly oxidized low density lipoprotein activates multiple apoptotic signaling pathways in human coronary cells. Faseb J 14:1996–2007.

Nara F, Tanaka M, Masuda-Inoue S, Yamasato Y, Doi-Yoshioka H, Suzuki-Konagai K, Kumakura S, Ogita T. 1999. Biological activities of scyphostatin, a neutral sphingomyelinase inhibitor from a discomycete, Trichopeziza mollissima. J Antibiot (Tokyo) 52:531–535.

Rzonca SO, Suva LJ, Gaddy D, Montague DC, Lecka-Czernik B. 2004. Bone is a target for the antidiabetic compound rosiglitazone. Endocrinology 145:401–406.

Spieker LE, Ruschitzka F, Luscher TF, Noll G. 2004. HDL and inflammation in atherosclerosis. Curr Drug Targets Immune Endocr Metabol Disord 4:51–57.

Suzuki O, Nozawa Y, Abe M. 2003. Sialic acids linked to glycoconjugates of Fas regulate the caspase-9-dependent and mitochondria-mediated pathway of Fas-induced apoptosis in Jurkat T cell lymphoma. Int J Oncol 23: 769–774.

Tani N. 2000. Development of selective low-density lipoprotein (LDL) apheresis system: Immobilized polyanion as LDL-specific adsorption for LDL apheresis system. 1996. Ther Apher 4:135–141.

Tanko LB, Bagger YZ, Christiansen C. 2003. Low bone mineral density in the hip as a marker of advanced atherosclerosis in elderly women. Calcif Tissue Int 73: 15–20.

Vasankari T, Ahotupa M, Toikka J, Mikkola J, Irjala K, Pasanen P, Neuvonen K, Raitakari O, Viikari J. 2001. Oxidized LDL and thickness of carotid intima-media are associated with coronary atherosclerosis in middle-aged men: Lower levels of oxidized LDL with statin therapy. Atherosclerosis 155:403–412.

Verrier E, Wang L, Wadham C, Albanese N, Hahn C, Gamble JR, Chatterjee VK, Vadas MA, Xia P. 2004. $PPAR_{\gamma}$ agonists ameliorate endothelial cell activation via inhibition of diacylglycerol-protein kinase C signaling pathway. Role of diacylglycerol kinase. Circ Res 94(11): 1515–1522.

Zagozdzon R, Bougeret C, Fu Y, Avraham HK. 2002. Overexpression of the Csk homologous kinase facilitates phosphorylation of Akt/PKB in MCF-7 cells. Int J Oncol 21:1347–1352.